Laboratori Nazionali di Frascati

C. Sanelli, A. Cattoni, L. Barbagelata, F. Crenna, M. Grattarola, G.C. Gualco and F.Rosatelli:

DESIGN OF A HYBRID PERMANENT MAGNET QUAD PROTOTYPE AS A POSSIBLE CANDIDATE FOR THE INTERSECTION REGIONS OF DAΦNE
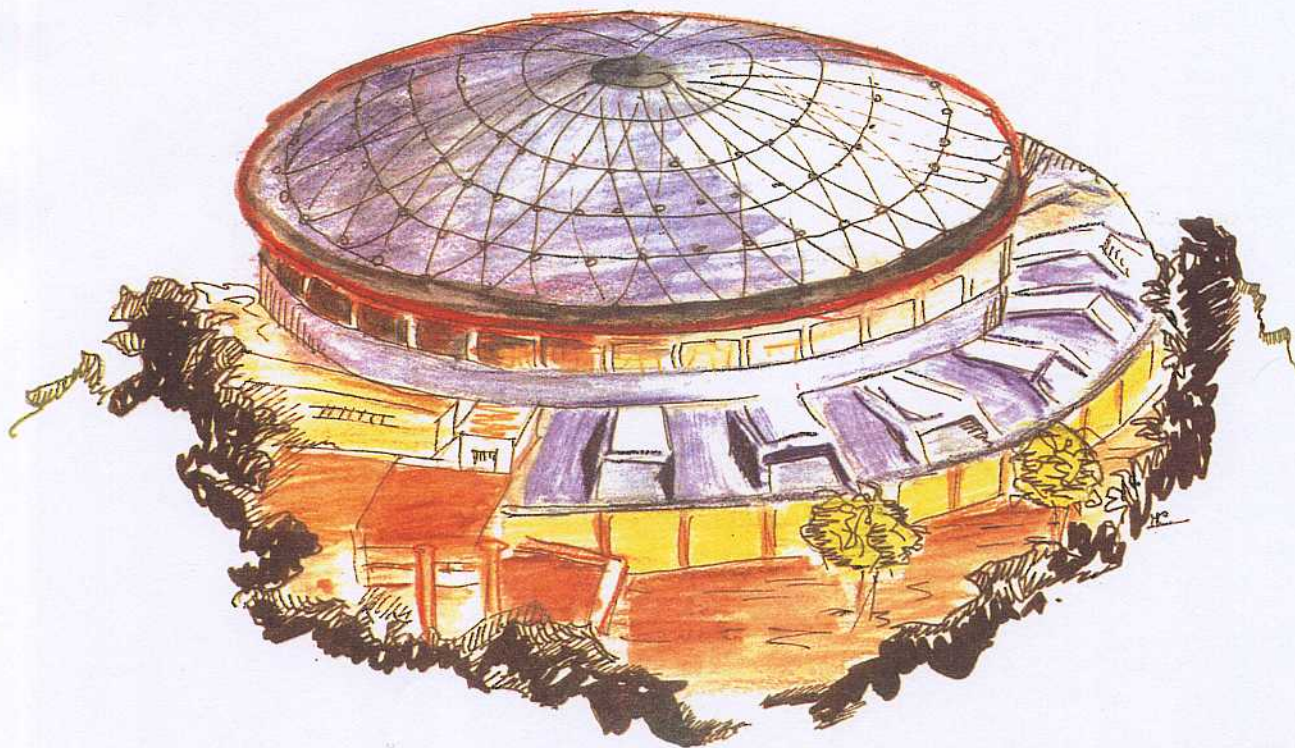
DESIGN OF A HYBRID PERMANENT MAGNET QUAD PROTOTYPE AS A POSSIBLE CANDIDATE FOR THE INTERSECTION REGIONS OF DAΦNE

C. Sanelli, A. Cattoni
INFN, Laboratori Nazionali di Frascati, Via E. Fermi 40, 00044 Frascati (Italia)

L. Barbagelata, F. Crenna, M. Grattarola, G.C. Gualco and F.Rosatelli
ANSALDO RICERCHE, Divisione Nuove Tecnologie, corso Perrone 25, 16161 Genova (Italia)

ABSTRACT

A hybrid, tunable, p.m. quadrupole prototype for Daφne has been designed and built in a collaboration between Ansaldo Ricerche –Genova and the Frascati National Laboratory Magnet Group. Magnetic calculation, constructive design and the first acceptance test results are briefly reported in this note. The leading ideas in conceiving this new type of mechanical set up, aimed to supply a magnetic lens with an iron dominated gradient quality and an effective possibility of easily adjusting the field profile and the magnetic length, are described. The large aperture radius compared to the very contained overall external dimensions of the yoke, make this type of magnet suitable for the low–beta insertions of the Daφne storage rings, where the large vacuum chamber acceptance needed and the very severe constraints imposed by the detectors, discourage the use of resistive or superconducting electromagnets. In addition a 15% tunability, only by actuating a couple of iron wedges per pole, gives to this quad the possibility of meeting the optimum gradient values that will be effectively known only after the commissioning of the machine.

1. - INTRODUCTION

In the Daφne Φ Factory, electrons and positrons circulate in two separate storage rings, whose top view is about elliptical, intersecting in the horizontal plane at an half–angle of 10 mrad, giving rise to two interaction points (I.P.), each one placed at the centre of a long straight section devoted to the experimental activities.

On both side of each I.P. a triplet of quadrupoles is needed, to focalize the beams and to obtain a minimum value of the β_y function at the I.P., which is a design parameter of paramount importance to achieve a high luminosity[1, 2, 3].

Likely every I.P. will be surrounded by a large detector incorporating the most of the straight section, vacuum chamber and the triplets of the low–beta insertion included.

In addition the first detector will be equipped with a big solenoid, may be superconducting, about 6 m in diameter and 5 m in length, whose magnetic field should not be seen by the machine beams (except for a short window of about ± 0.5 m around the I.P.). This means that shielding solenoids, coaxial with the beams are needed[4], limiting even more the allowance for the low–beta insertion quads, given also the fact that the detector wants to cover as maximum as possible of the solid angle.

2.-BOUNDARY CONDITIONS FOR THE LOW–BETA INSERTION QUADS

2.1 – The detector requests, aimed to maximize the solid angle, impose to confine the machine components, shielding solenoids included, in a conical zone with the vertex centred in the I.P. and a half aperture angle of 8.5 degrees. Taking into account the machine optics lay–out, this comes out in the following constraints for the overall radial extension of the quads:

– First quadrupole, the closest to the I.P., outer radius ≤ 0.067 m.

– Third quadrupole, the farthest from the I.P., outer radius ≤ 0.156 m.

With the above radial extensions a shielding current sheet would not be allowed for the entire length of the first quad, but would be easily accommodated to cover the remaining length of the conical zone.

2.2 – The machine optics requests concern the gradient intensity, the field quality and the beam stay clear needed in the good field zone; more over the crossing at an angle imposes a separation to the beams in the horizontal plane, increasing with the distance from the I.P., so that the optics requests are even more stringent and the lens aperture more critical. Also other points of view should be taken into account dealing with the vacuum chamber conductance (the lumped pumps should be installed outside the detector so that they are located far away from the I.P. where, on the contrary, the best of the vacuum is needed), and also dealing with the energy loss and the energy spread that can be produced in a bunch passing through any beam pipe discontinuity. This last argument comes from a detector requests to enlarge the pipe diameter in the window zone surrounding the I.P. so that a tapering of the vacuum chamber is needed[5] to

reduce the bunch energy spread. Reducing the slope of the tapering, that can be obtained increasing both the taper length and the minor diameter extension at the transition between the two cross sections, (obviously one would like having no transition at all) helps very much. This is why the inner radius of the low–beta insertion quads should be as large as possible.

2.3 – The above considerations have pointed out two contradictory conditions: the ideal low–beta insertion quads should have, for the wanted field gradients (see Table I) , an aperture as large as possible and no cross sectional variation of the vacuum chamber in spite of the overall radial extension imposed "a priori" by the detector. Table I gives also the following parameters for the low– beta insertion region:

– s: distance from the I.P. of the magnetic edge of each quadrupole, taken along the ideal orbit.

– R_2:   overall radial extension allowed at the edges of each quad; this value takes into account the limitations imposed by the shielding solenoid and by the mechanical supporting and centring systems .

– $10.\sigma_x$:   this value takes into account the machine dynamic aperture and the radial r.m.s. bunch width for a gaussian distribution of particles.

– Δx: half separation between the beam centres.

– L: allowance for the vacuum pipe thickness, the assembling tolerance and the baking panel.

– r_1:   the resulting minimum aperture radius needed for each quadrupole.

TABLE I

	s (m)	R_2 (mm)	$10.\sigma x$ (mm)	Δx	L (mm)	r_1 (mm)	(mm)	G (T/m)
Q1	.45		21.3	4.5		31.8		
		67.			6.		}32.	7.4
	.63		19.9	5.94		31.84		
Q2	.76		17.9	6.71		30.61		
		85.5			6.		}38.	11.9
	1.1		19.8	11.9		37.7		
Q3	1.23		23.3	15.3		44.6		
		156.			6.		}54.	6.71
	1.51		27.1	20.1		53.2		

Notice that, for each quadrupole, r_1 and R_2 are taken constant to avoid any supplementary complication in building quads with the inside and outside radii varying linearly.

From a design point of view three possibilities could, in principle, be investigated:

- resistive quads with soft iron yokes and electrically powered coils, water–cooled;
- superconducting quads, contained in their cryostats, cooled by liquid helium;
- permanent magnet quads (full p.m. or hybrid, possibly tunable).

From the geometrical limits and the specified gradients reported in Table I, it is clear that Q1 and Q2 can't be conventional or s. c. quadrupoles; but, in addition to the above mentioned space limitations, there is the general requirement that the adopted solution should be according with an easy handling and operation of the detectors. No risk should be taken of any leakage of current, water, gases, vacuum, no risk of any possible damage to the internal components, belonging to the quads or to their feeding plants, is acceptable, so that the complicated and time consuming operations of opening the huge detector should be absolutely avoided.

Bearing this in mind and having available in our storage a stock of about 500 prismatic Recoma Magnets, 9x9 mm^2 in cross section, 70 mm in length, we came to the decision of trying a hybrid permanent magnet quadrupole, just to learn what were the possibilities of solving our problems.

In order to avoid possible misunderstandings, it must be immediately pointed out that our aim was essentially to get, as soon as possible, something ready for measurements to help for a final decision. After some very preliminary calculations, it was clear that the shape and geometry of the existing permanent magnets was not the optimum solution to effectively build anyone of the low–beta insertion quads; for example the segmentation in steps of 70 mm made impossible to fit the prescribed magnetic lengths; even more, the number of existing p. m. was too small compared to the necessity of achieving a high uniformity in terms of easy axis orientation and field strength to get the prescribed gradient intensities.

After few tentative solutions it came out that we could approach the geometry of Q3 but with a magnetic length in excess and an aperture radius and a field gradient in defect. This is what we did in spite of the above mentioned deficiencies, because the magnet to be built was certainly very suitable to fully learn the magnetic behaviour and the mechanical problems of a hybrid p.m. quad for the low beta insertion of Daϕne.

Last but not least consideration: the I.P. structure of the machine should be designed in collaboration with the detector Group in the sense that the effective optimum solution will have to optimize the detection efficiencies for a given machine luminosity; for instance an increase of the 8.5 degrees, the conical zone allowed to the machine components, would reduce the solid angle accepted by the detector but, a part the advantages for solving some mechanical problems of the quads, (supports, alignment, compensator solenoids and so on), would give the possibility of increasing the lens apertures and the beams separation which would allow storing more bunches and increasing the machine luminosity. At present the I.P. quads scenario can still be changed so that we did not fill forced to fit exactly, in the prototype phase, the mechanical dimensions of one component; more advantageous was to save time and money getting technological and physical answers as soon as possible.

3. – BASIC IDEAS

As it is known[6, 7], full p. m. quads, made with modern compounds, can achieve, on a given bore radius r, field gradients up to about 2/r (Tesla/m). This is true if one can put enough active material around the lens aperture (outer radius R » r) and if, for instance, p.m. pieces of trapezoidal shape, with five different orientations of the easy axis, are available to build a 16–pieces quadrupole. More realistically, because one wants to build p.m. quads very compact, putting R=4r only, one can still get, at the aperture, a magnetic field of about 1.4 Tesla, when, on the contrary, for a high quality conventional quadrupole is already difficult to reach 1 Tesla at the pole profile.

Some tricks have been proposed also to make full p.m. quads tunable, adding to the basic structure some other shaped p.m. symmetrically moved.

In our real situation, having 500 prismatic Recoma magnets not shaped at all (square cross section), having only one easy axis orientation, the way to follow should be obviously different: our permanent magnets could be more usefully applied as flux generators in a sort of conventional quad where the coils are replaced by some arrays of p.m.

This is what we actually did, coming to the construction of 4 flux generators, resulting each one in an approximately square cross section box of 4 cm side and about 28 cm in length, containing 64 p.m.; (in total 256 pieces of p.m. utilized over 500 available).

It is clear that the above number is the maximum allowed for a reasonable choice, in order to achieve an acceptable uniformity in terms of easy axis orientation and field strength of the flux generators.

We planned to treat the flux generators like coils, but there are at least two fundamental drawbacks: electrical coils can be built very equal one with respect to the other and, being powered in series, they can give, in principle, equal contributions to the magnetic field in a system like a fully symmetric quadrupole; second, there is a single current to tune the field. This was not the case of our flux generators in spite of the accuracy of the p.m. characterization and the "sorting" program applied to insert the p.m. into their boxes with a sequence aimed to maximize the flux generators uniformity. Applied procedure and results will be described in a following paragraph; here we want simply to point out that it was envisaged the necessity of having a mechanical tuning capability, not only to set the gradient value but also to compensate the flux generators inequalities. The quadrupole symmetry and the mechanical arrangement have suggested to apply two tuning studs, wedge shaped, per pole, independently movable. In addition ,the iron poles, far from saturation, would act as flywheels able to smooth even more the effects of possible differences, among the flux generators, in terms of resulting easy axis orientation and field intensity.

Based on the above described ideas, our hybrid quad, shown in Fig. 1, was expected not too far from an iron dominated electromagnet, whose field quality could be always improved correcting the pole profile.
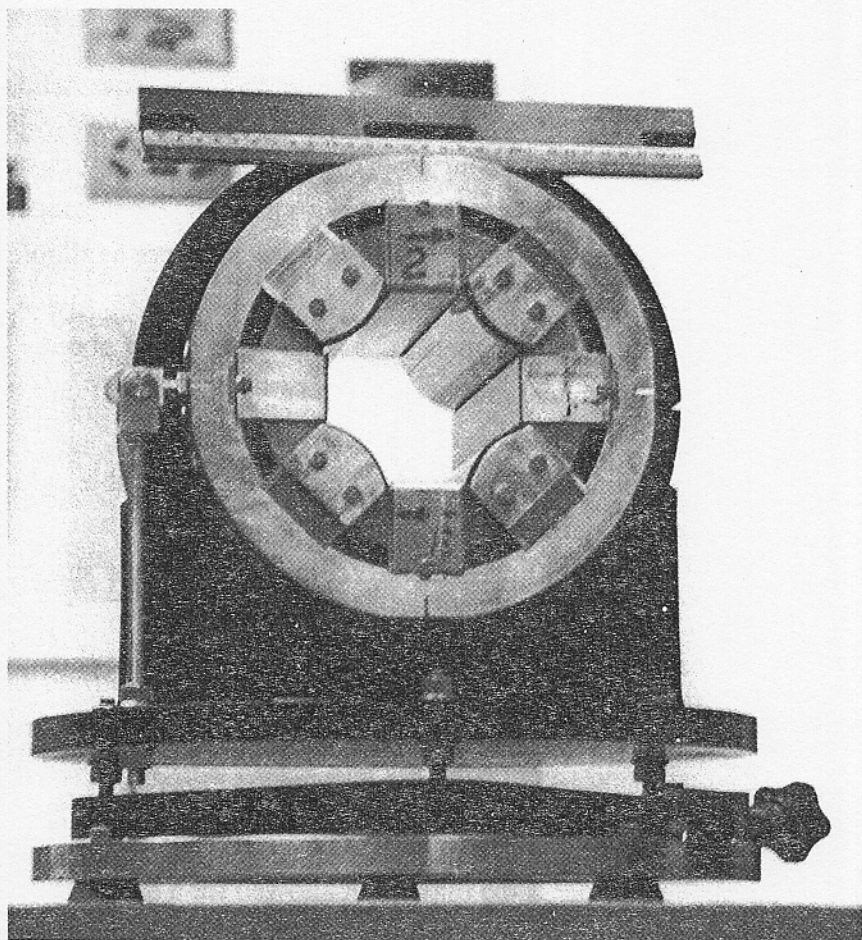
FIG. 1 – The hybrid, tunable, permanent magnet assisted quadrupole.

4 – MAGNETIC CALCULATIONS

The magnetic calculations have been performed by means of different computer codes. The hybrid quadrupole geometry has been analyzed with PANDIRA (2D–code) at LNF and with PE2D and TOSCA at Ansaldo (2D and 3D codes respectively).

Pandira and PE2D gave nearly the same results but the 3D analysis gave quite different results.

The basic geometry has been carefully studied and modified to obtain the maximum gradient.

At the beginning we set the radial length of the iron wedge the same of that of the p.m blocks. The calculations showed that there is (like on the p.m. undulators[8]) a gradient increase of the order of 3 % when the p.m. block is overhanging the wedge. Consequently we decided to shorten the wedge length, decreasing at the same time the fringing field outside the quadrupole.

Even the position of the permanent magnets was optimized to get a higher gradient, moving the p.m. blocks toward the quadrupole centre. Note that when this distance is too much reduced, the flux going out from the p.m. block closes on itself and it does not penetrate into the iron, so that one loses the 'iron dominated' condition.

Taking into account all these considerations the Pandira run predicted a gradient of 5.74 [T/m]. It must be specified that in this simulation the pole profile was approximated with an arc of circle.

The calculations made at Ansaldo by means of PE2D showed nearly the same results, 5.84 [T/m] with circular pole profile and 5.67 [T/m] with hyperbolic pole profile. The last profile had the advantage to reduce the gradient variation from 8 to 3 * 10^{-3} at 12 mm far from the quadrupole centre.

Fig. 2 shows the basic geometry with the wedge closed, while Fig. 3 shows the flux line path from Pandira for the same geometry with the wedge opened. ·

Fig. 4 shows the gradient variation as calculated by Pandira with the wedges closed and opened respectively.

The Tosca calculations, made at Ansaldo, gave results strongly different from the 2D codes. The predicted value at the centre of the quadrupole was 4.87 [T/m]. Fig. 5 shows the gradient homogeneity $\Delta G/G_o$, where G_o is the gradient at the quadrupole centre.
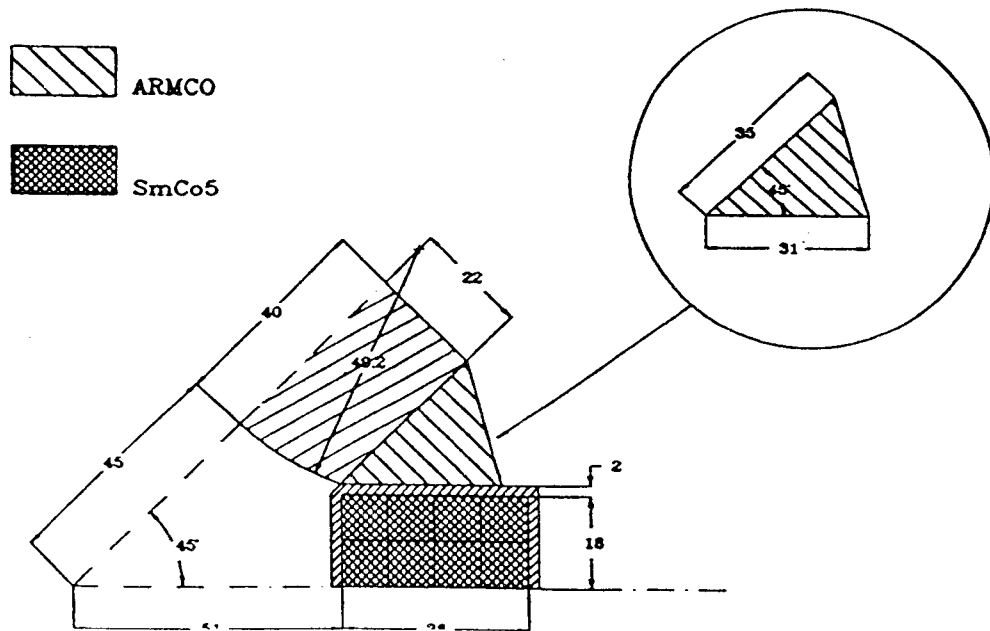
FIG. 2 – Hybrid quadrupole basic geometry (1/8th).
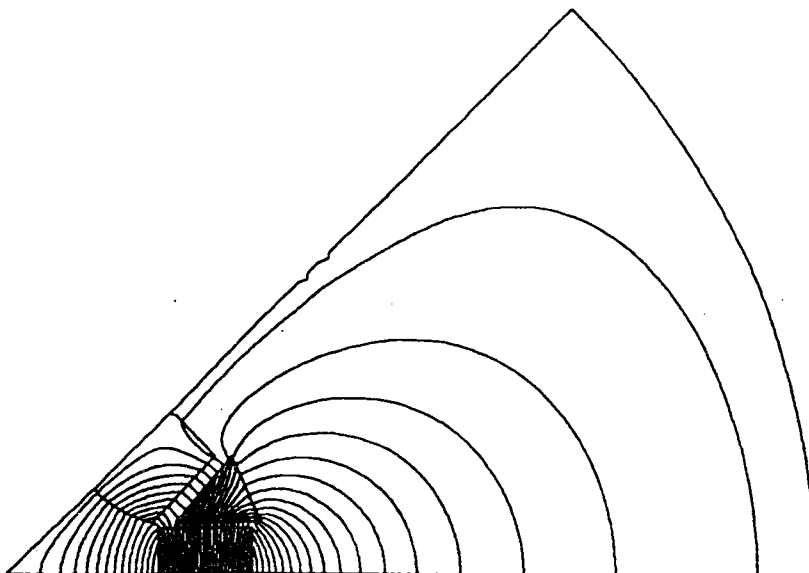
FIG. 3 – Flux line path for the geometry in Fig. 2 from PANDIRA.
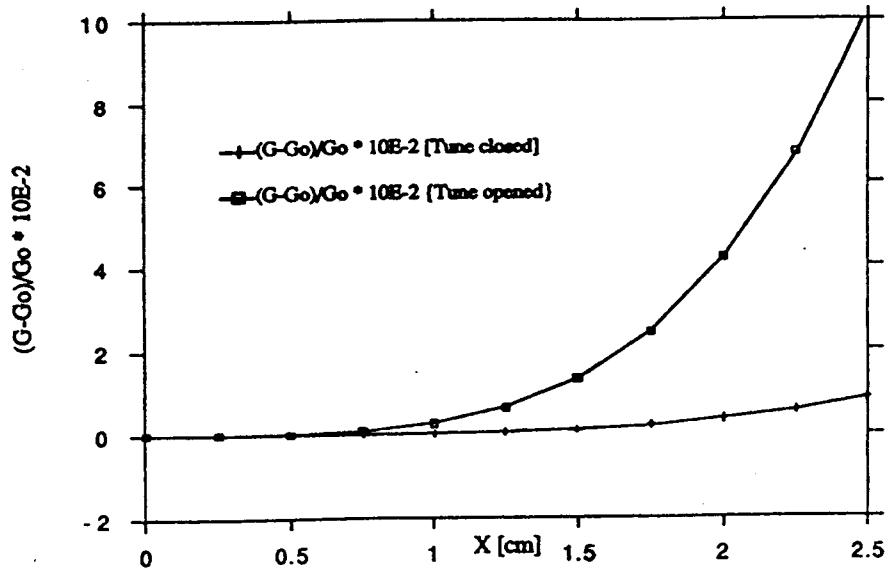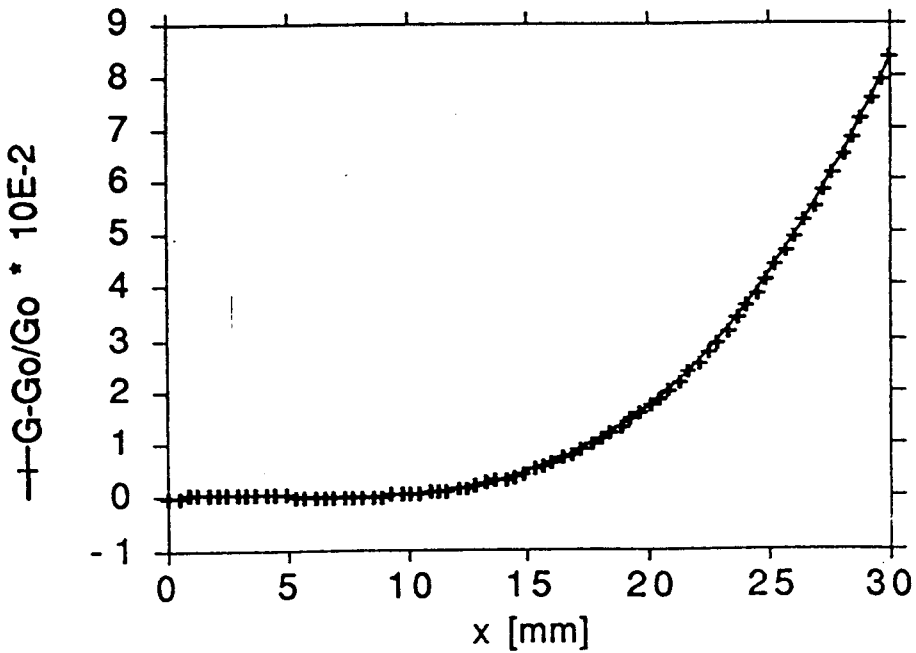
FIG. 4 – Gradient uniformity from PANDIRA.

FIG. 5 – Gradient homogeneity on the horizontal axis at the quadrupole midplane as predicted by TOSCA.

5 – PERMANENT MAGNET MEASUREMENTS AND SORTING

5.1 PERMANENT MAGNET MEASUREMENTS

The characterization of the permanent magnets for the quadrupole has been carried out in three steps:

1) Preliminary characterization by a Hall effect gauss–meter

2) Dimensional measurements

3) Measurements of the angular deviation and of the relative strength of magnetization.

The aim of the first step was to pick out and discard magnets damaged or whose magnetic characteristics were too far from the average values.

A total of 568 permanent magnets have been measured. The average measured magnetic field has been : $B_{average}$ =0.281 Tesla with standard deviation 0.008 Tesla.

Only 426 magnets were chosen, in conformity with $0.27 \leq B \leq 0.29$ Tesla. Fig. 6 shows the distribution of the measured magnets.

The selected magnets were then dimensionally measured and the magnets whose transverse dimensions differed from the nominal value (9 mm) by more than 0.05 mm have been discarded. 397 magnets have been accepted having an average height and width of 9.0 mm with standard deviation 0.01 mm, and an average length 70.07 mm with standard deviation 0.02 mm. Figs. 7, 8 and 9 show the gaussian distribution of the magnet height, width and length.
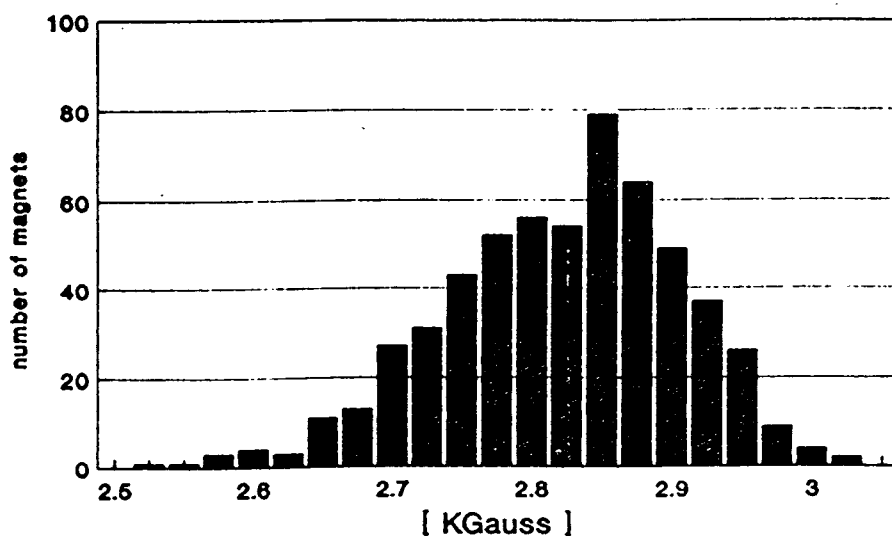

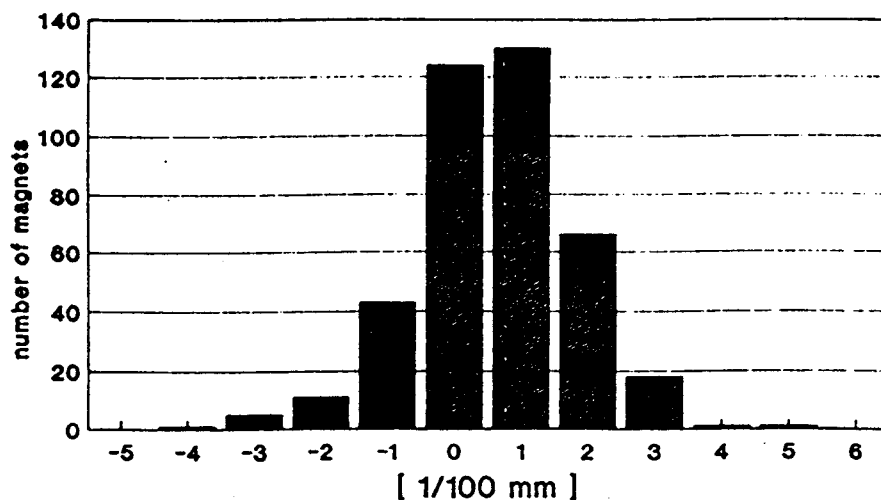FIG. 6 – P.m. field intensity distribution.
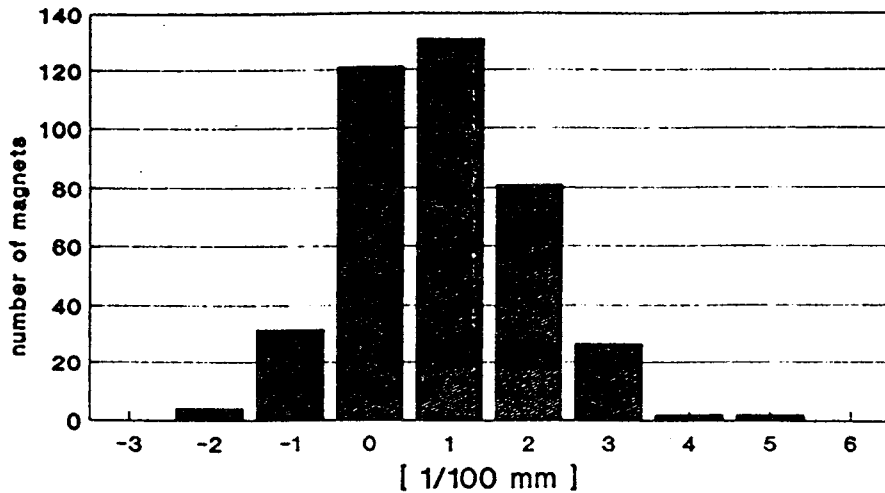

FIG. 7 – P.m. mechanical height distribution.

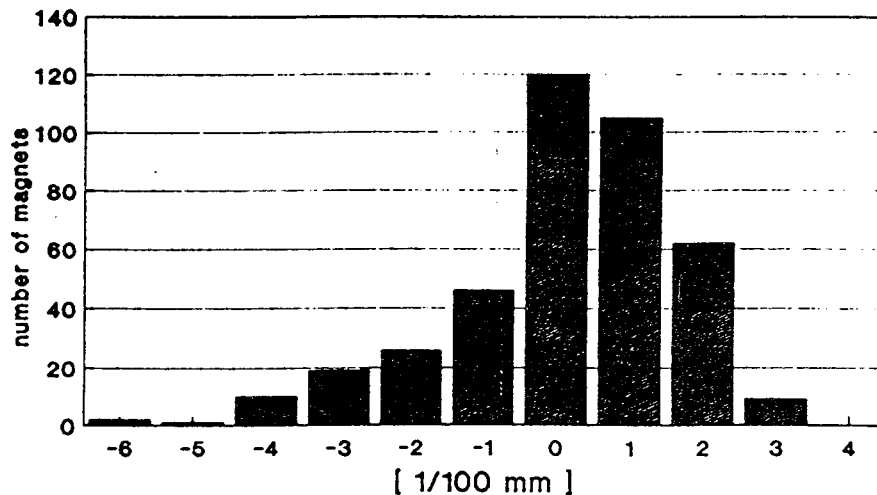FIG. 8 – P.m. mechanical width distribution.

FIG. 9 – P.m. mechanical lenght distribution.

These magnets have then been magnetically characterized. The equipment set up at Ansaldo Ricerche, allows to measure the relative strength of magnetization (with respect to a reference magnet) and the angular deviation of magnetization from the nominal direction. The nominal direction is defined as the vertical axis perpendicular to the reference magnet face. The magnet to be measured ($|M|$) and the reference magnet ($|M_r|$), both with parallel and anti-parallel magnetic moments, are kept in rotation inside the bore of a coil at a frequency of 1200 turns/minute. An harmonic analysis (FFT) of the induced voltage allows to obtain the amplitude and the phase of the fundamental and then the ε and θ values (where ε is defined as ($|M| - |M_r|$) / $|M_r|$ and θ is the angular deviation of the magnetization with respect to the reference one). The experimental errors are: $\pm 10^{-4}$ for ε and ± 1 mrad for θ. For the best precision of the successive measurements the reference magnet must have the following characteristics:

– $|M|$ as close as possible to the average value.

– θ as small as possible.

After the preliminary magnetic characterization, 13 magnets, whose $|M|$ and θ were as close as possible around the distribution centre, have been chosen and 12 of them have been

measured with respect to an arbitrary magnet, then, among these, the magnet number 186 was picked out for final reference. 396 magnets have been measured with respect to that magnet and the following results were obtained:

-    standard deviation of ε = 0.014,
-    standard deviation of θ = 0.010 rad.

Fig. 10 and 11 show the relative strength and angular deviation distribution of the permanent magnets.
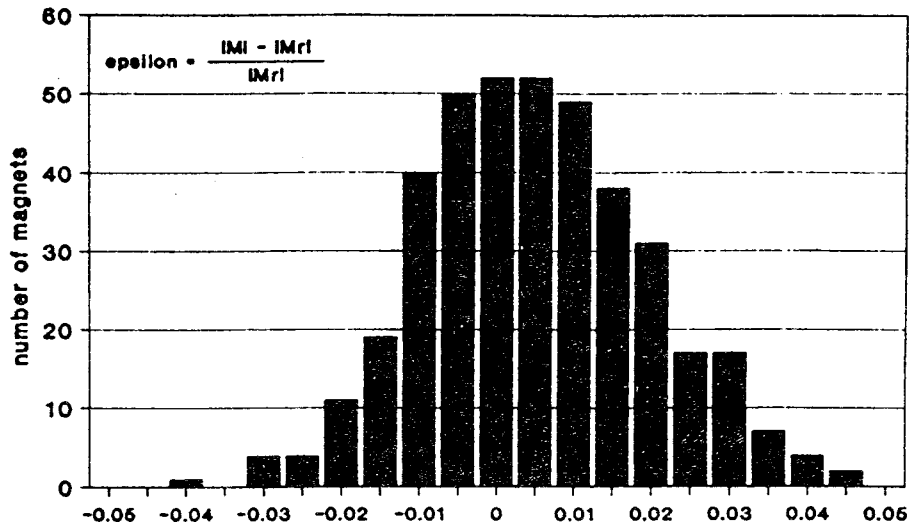
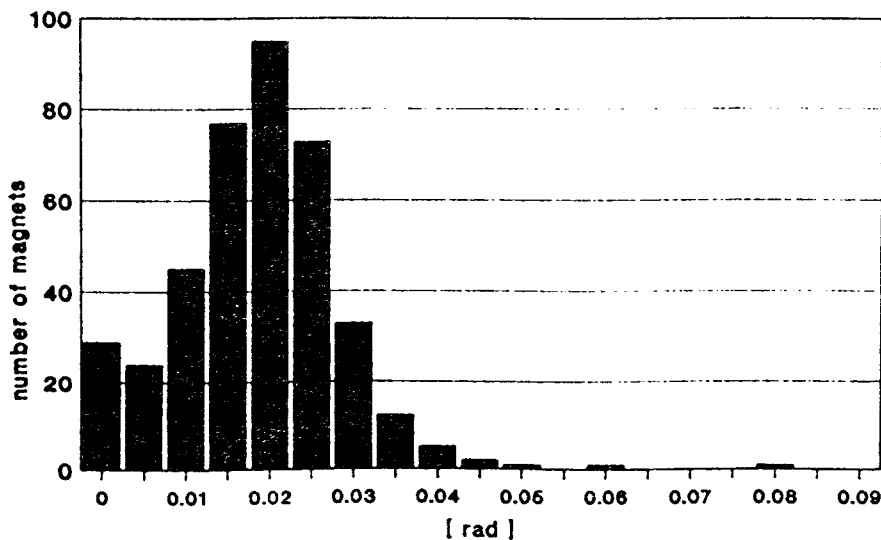FIG. 10 – P.m. relative strenght distribution.

FIG. 11 – P.m. angular deviation distribution.

5.2 SORTING OF THE PERMANENT MAGNETS

The hybrid quadrupole needs four flux generators, four layers of 16 magnets each, for a total of 256 permanent magnets. Because magnets arranged in symmetrical position with respect to the plane shown in Fig. 12 have the same importance with regard to the final performance of the quadrupole, sorting has been carried out forming 8 groups of magnets, 32 magnets for each group. The magnets of the same group are as similar as possible among them, both in regard to ϵ and to θ. The first group is composed of magnets whose θ and ϵ are as small as possible and so on for the second and the others. This first group has been arranged in position 1 and 2 in Fig. 12, second group in position 3 and 4 and so on. Each 32 magnet group has at its time been divided in 8 groups, 4 magnets each, as similar as possible. The 4 magnets have been mounted one behind the other to obtain the best longitudinal homogeneity. A specific Turbo–Pascal code has been developed for sorting. The code reads the relative strength of the magnetization and the angular deviation of 396 measured magnets and groups them using the 256 best permanent magnets.

Following up this way an assembling map has been compiled for the four flux generators.
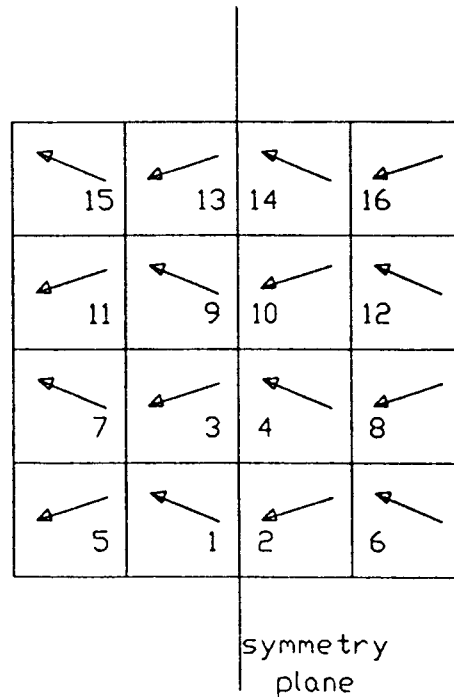

FIG. 12 – Ideal positioning of the selected p.m. groups inside the flux generators.

5.3 – FLUX GENERATOR MEASUREMENTS

One time the four flux generators have been assembled, they have been magnetically tested using a Hall effect Gauss–meter. The Hall Probe was put at 29 mm from the permanent magnets surface and it was moved longitudinally along four lines parallel to the quadrupole axis, two above and two below the flux generator surfaces, and the magnetic field was recorded. In addition a map along a transverse axis, at the same distance from the magnets surface, in correspondence of the flux generator mid–plane, has been carried out. Fig. 13 shows a typical comparison of the measured fields along the longitudinal directions. Fig. 14 shows the magnetic field comparison along the transverse direction.

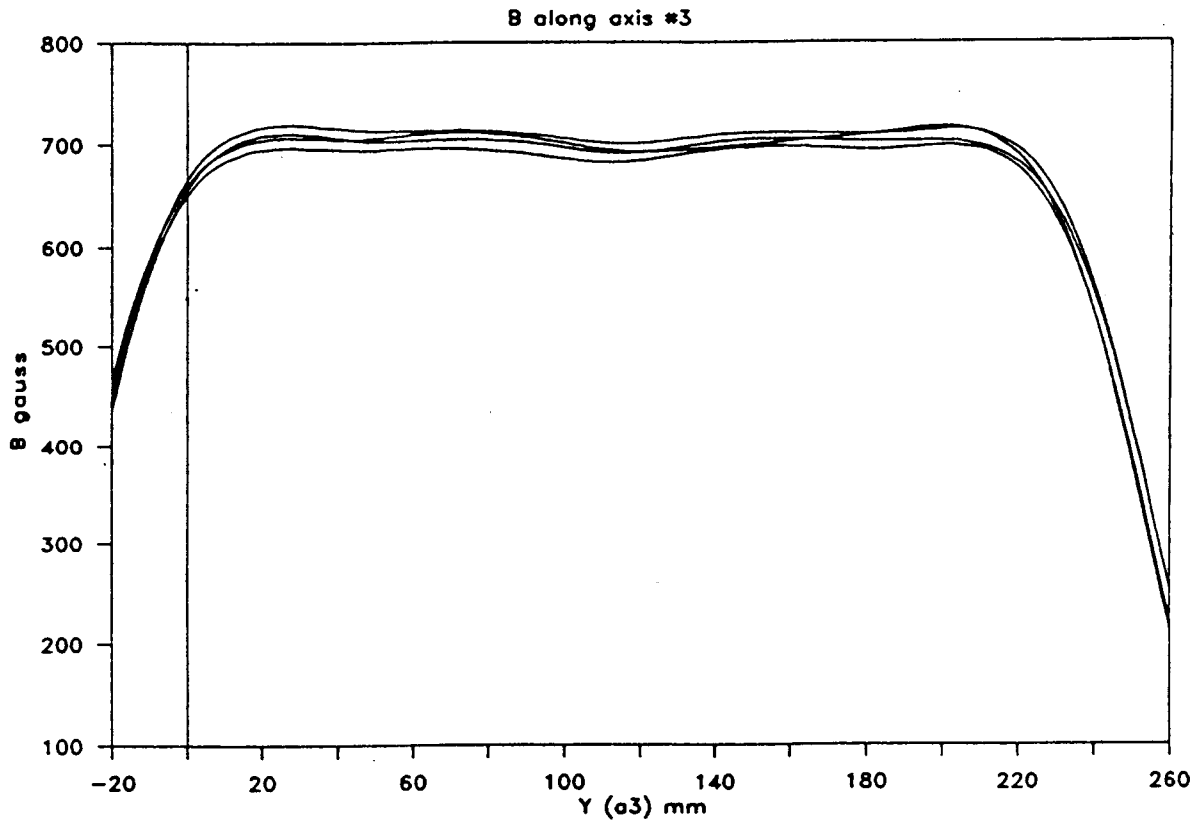The maximum deviation among the four flux generators is about 4 %.

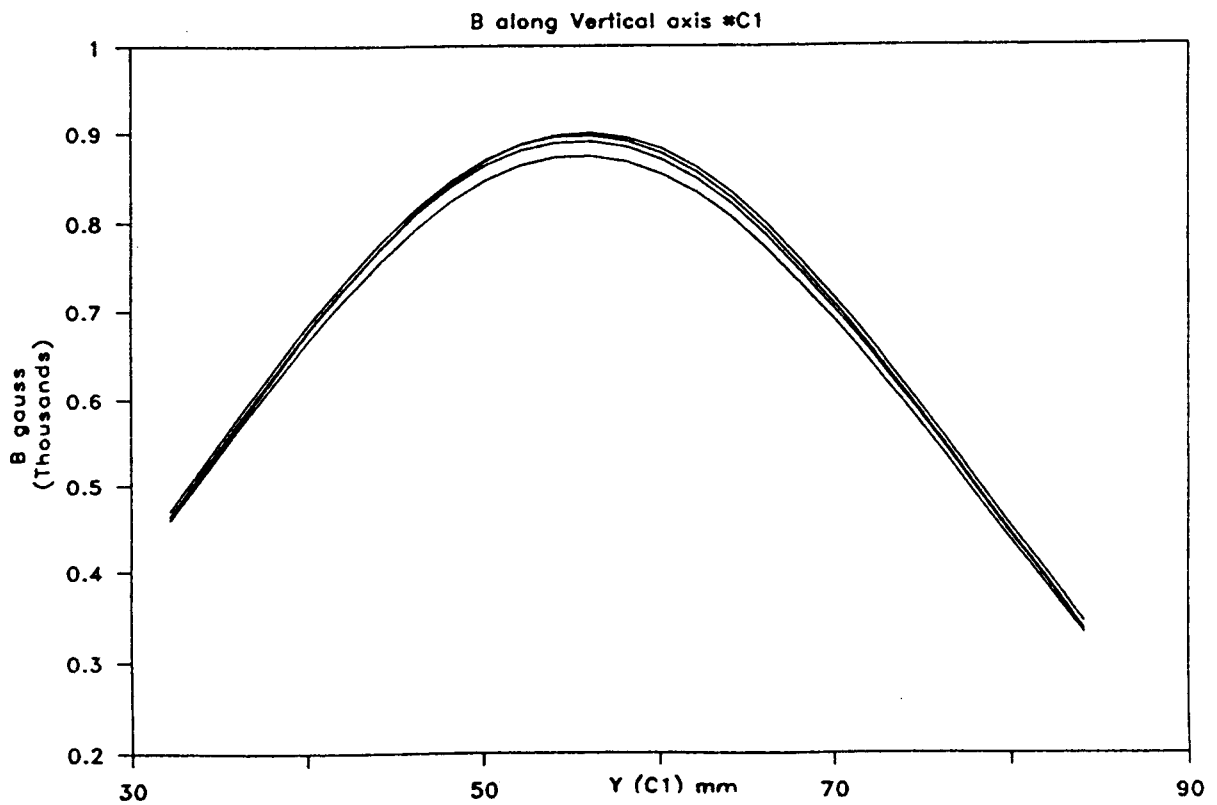FIG. 13 – Comparison of the magnetic fields measured along the longitudinal direction of the flux generators.

FIG. 14 – Comparison of the magnetic fields measured along the transverse direction at the midplane of the flux generators.

6. – MECHANICAL DESIGN

6.1 – GENERAL

The quadrupole prototype is essentially composed by four poles, four magnet assemblies, above defined as flux generators, and eight tuning studs (wedges), all supported by an outer cylindrical structure. Each pole is fixed to the structure by means of two pins and two bolts. Calibrated spacers of different thickness can be placed on the pole back in order to be able to change the bore radius. Each magnet assembly is made up by magnet blocks not glued but mechanically clamped by an external aluminum structure. The four magnet assemblies are mounted in calibrated slots in the outer cylindrical structure and fixed by means of three bolts. The movable tuning wedges slide on the lateral sides of the magnet assembly boxes. Two calibrated pins and two driving screws provide the correct alignment and movement for each tuning wedge. The gap between the tuning wedges and the poles can be set from 0 to 4.5 mm. The outer cylindrical structure was designed to allow the splitting of the quadrupole in two parts for mounting operations around the vacuum chamber. The correct assembly of the two parts is guaranteed by four conical pins and six bolts. An adjustable mechanical support to align the quadrupole with the measuring bench and a specific device for opening and closing of the quadrupole with the required tolerances were designed and realized. The opening–closing operations cannot be done by hands cause the magnetic forces between the two parts. Fig. 15 shows the mechanical lay–out of the hybrid quadrupole.

6.2 – MECHANICAL CALCULATIONS

A detailed analysis of the magnetic forces acting on all the components was performed. The calculations were carried out in 2D approximation (conservative condition) using PE2D code (Maxwell Stress Tensor Method). The analysis has shown that the forces acting on the components are quite low, from the structural point of view, but high enough to make the hand assembly difficult and dangerous for the operators. On the basis of these results a complete set of assembling tools was designed and realized. A final finite element stress analysis (ANSYS 4.4 code) has shown the good stiffness of the external cylindrical structure under the magnetic loads (maximum calculated displacement $0.9*10^{-7}$ m).

6.3 – MATERIALS

The following materials have been used for the different quadrupole parts :

– Magnet assemblies : SmCo5 magnet blocks with nominal residual field Br = 8.5 kGauss and coercive force Hc = 8300 Oe.

– Poles and tuning wedges: ARMCO pure iron (99.7 %).

– Outer cylindrical structure: ERGAL aluminum alloy.

– Screws and bolts: AISI 304 stainless steel and brass.

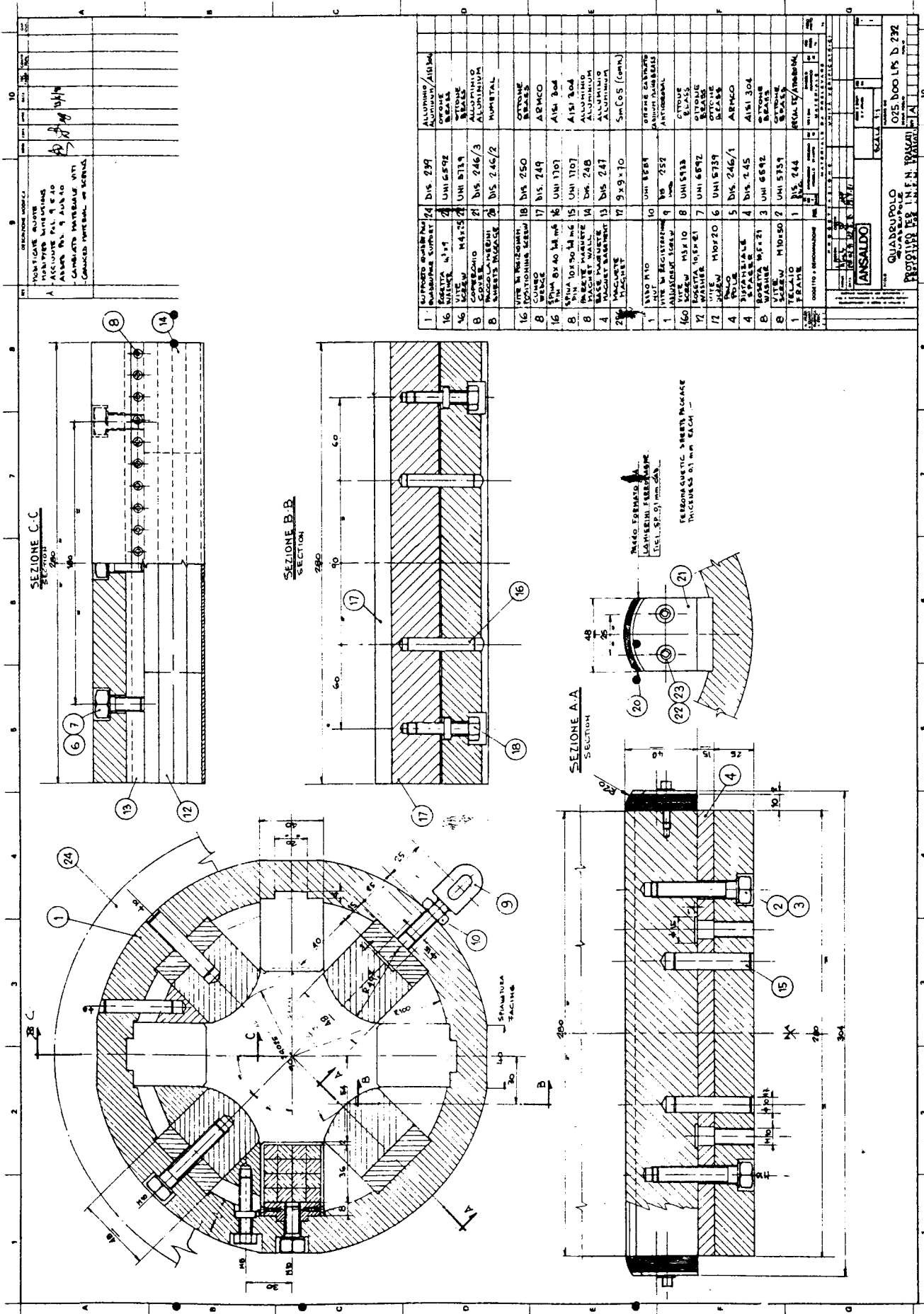– Pins: AISI 304 stainless steel.

FIG. 15

6.4 – MACHINING

Machining tolerances, material stabilization and an accurate assembly are critical issues for the achievement of the final dimensional and shape requirements. The two parts of the cylindrical structure were obtained from a massive extruded bar. After a pre–machining they were heat treated for stabilization and then finished on the contact surfaces, pinned and bolted each other. The whole assembly was then finished machining to obtain the final structure. A dedicated machining device was designed and realized for the final grinding of the calibrated slots for poles and permanent magnet assemblies. Also the iron poles and tuners were first pre–machined, heat treated (vacuum furnace at 1200°C for two hours) and then finished.Specific tests were carried out to estimate the deformations due to the heat treatments in order to pre–machine as close as possible to the final dimensions and minimize the finishing work. The pole profile was realized by means of a numerical control machine. The external box of the permanent magnet assembly was too thin to be machined so that the final grinding was made after the magnet block assembling to avoid any heating of the magnetic material.

6.5 – ASSEMBLY

The two more interesting phases of the quadrupole fitting up were the assembling of the flux generators and of the whole magnetic structure inside the outer cylinder.

Concerning the flux generators, a particular assembly device was realized to allow a mechanical clamping without any glue.The magnets mounting was quite delicate cause the magnetic forces and the brittleness of the magnet blocks. An assembly tool was realized to guide the permanent magnet assemblies into their slots, by means of driving screws, preventing all lateral movements and rotations due to magnetic forces.

As a first operation,the tuning wedges were mounted, with their guiding pins and driving screws, on the outer cylinder. The poles were then bolted on precision flat surfaces and two pins provide their alignment. Finally the flux generators were inserted.

All the dimensional and mechanical tests were performed before the magnets mounting in order to avoid all the problems connected to the interactions between the magnetic field and the measuring equipment. All the assembly operations were carried out in controlled environment (20°C).

6.6 – POLE PROFILE OPTIMIZATION

A parametric magnetic analysis was performed to optimized the pole profile. The calculations were performed in 2D geometry by means of the PE2D code (Vector Field). The pole profile was described by means of an analytic curve,changing during the optimization, in order to simplify the generation of the mesh. An hyperbolic profile was chosen. The optimization was performed changing the hyperbole parameters, keeping the bore radius constant, in order to minimize the relative gradient variation $\Delta G = (G\text{–}Go)/Go$ at 20 mm from the quadrupole centre (G = local gradient; Go = gradient in the centre). The optimization started with the theoretical pole profile:

$$y(x) = Ro^2 / 2\,x$$

where Ro = 45 mm is the bore radius and only those profiles compatible with the geometrical and the assembling constraints were taken into consideration. The ΔG value was decreased from $8.13*10\text{–}3$ to $2.92*10\text{–}3$ with the profile:

$$y(x) = (h*x+a-h^2)/(x-h)$$

where: $a= 700$ mm^2, $h=5.362$ mm. ($20 \leq x \leq 50$ mm)

6.7 DIMENSIONAL TESTS

The dimensional tests were performed by means of an INSPECTOR MIDI OCN (1984) with RENISCHAW probe in controlled environment (20 °C). All the singular components were tested and the dimensions of the quadrupole assembly were verified. The alignment of the assembled pole was found in the given tolerances. The parallelism and the distance of the poles were within 0.05 mm and their reciprocal perpendicularity within 0.02°.

7. – MAGNETIC MEASUREMENTS

A first set of magnetic measurements has been performed by means of a Hall effect Gauss–meter at Ansaldo Ricerche.Field maps on the horizontal and vertical axes laying on the medium transverse plane and on the planes in front and on the back of the quadrupole, for different wedge positions, have been carried out. In addition, field integral maps along lines parallel to the longitudinal axis at ±16, ±18, ±20, ±22 and ±24 mm from the quadrupole centre on the horizontal and vertical axes have been recorded. Finally, the fringing field outside the magnet has been measured and the relative curves plotted.

For obvious reasons only a few curves are reported here.

The average measured gradient with the wedges closed is 5.268 T/m. The gradient with the wedges completely opened is 4.574 T/m. This allows a tune range of 13.2%. The maximum measured gradient value is –8.2 % lower than the Pandira calculation and +8.1 % greater than the Tosca evaluation.

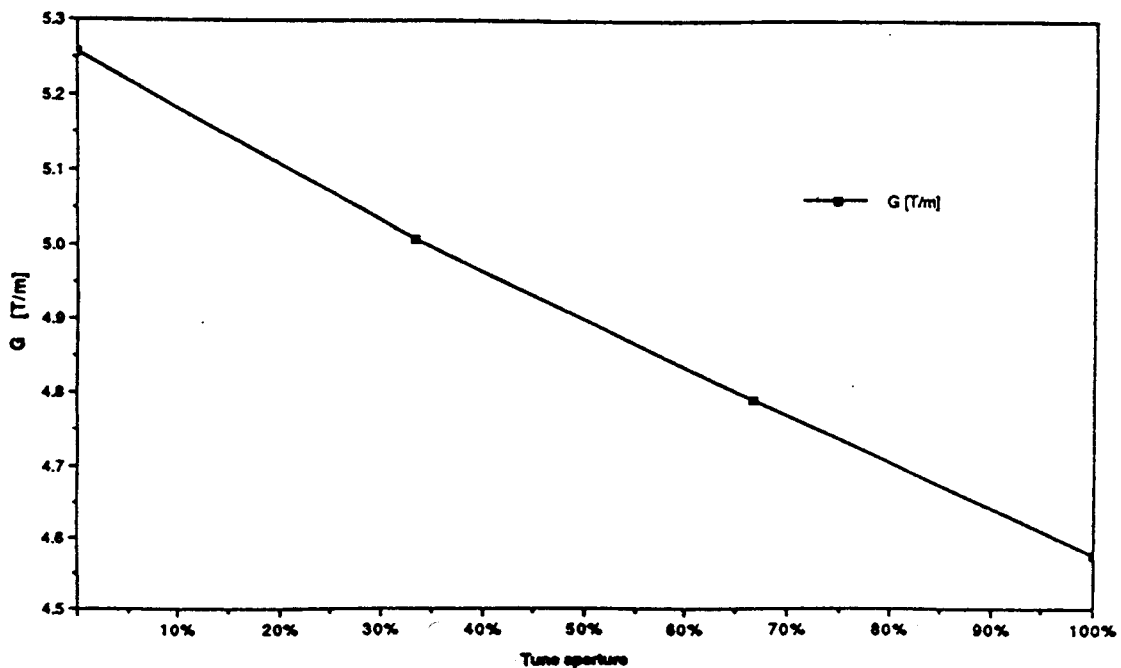Fig. 16 shows how the gradient decreases opening the wedges.

FIG. 16 – Absolute gradient variation vs tuning wedge position.

The magnetic length of the quadrupole has been calculated using the field integral maps. The average value, on a total of 20 curves, is 338.74 mm ±0.4 mm. Fig. 17 shows the field variation along an axis parallel to the quadrupole axis but horizontally shifted 20 mm from the quadrupole centre.

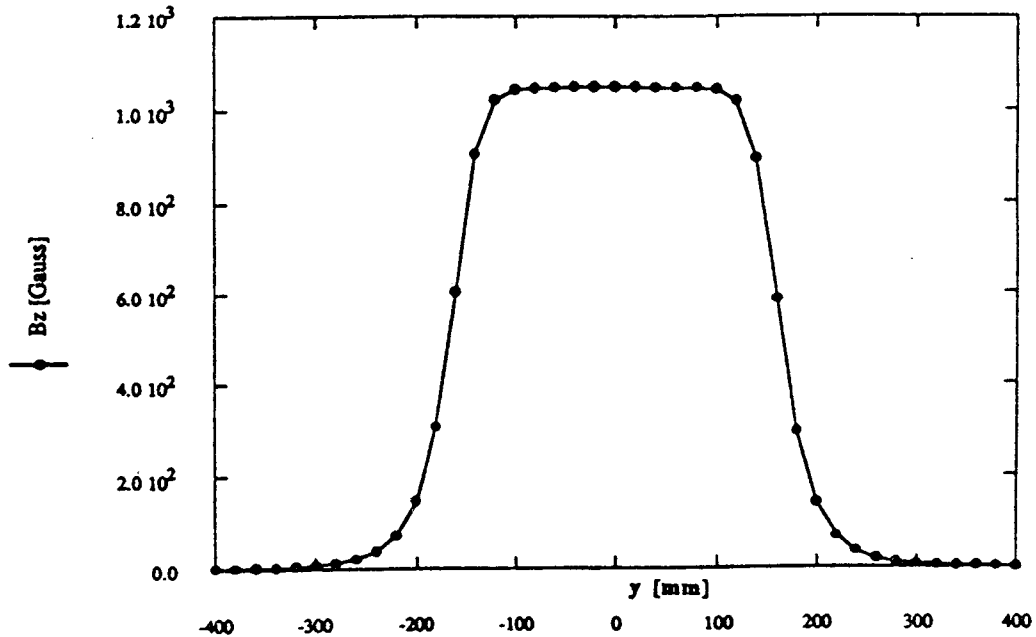**FIG. 17** – Longitudinal field profile along an axis 20 mm horizontally shifted from the quad axis.
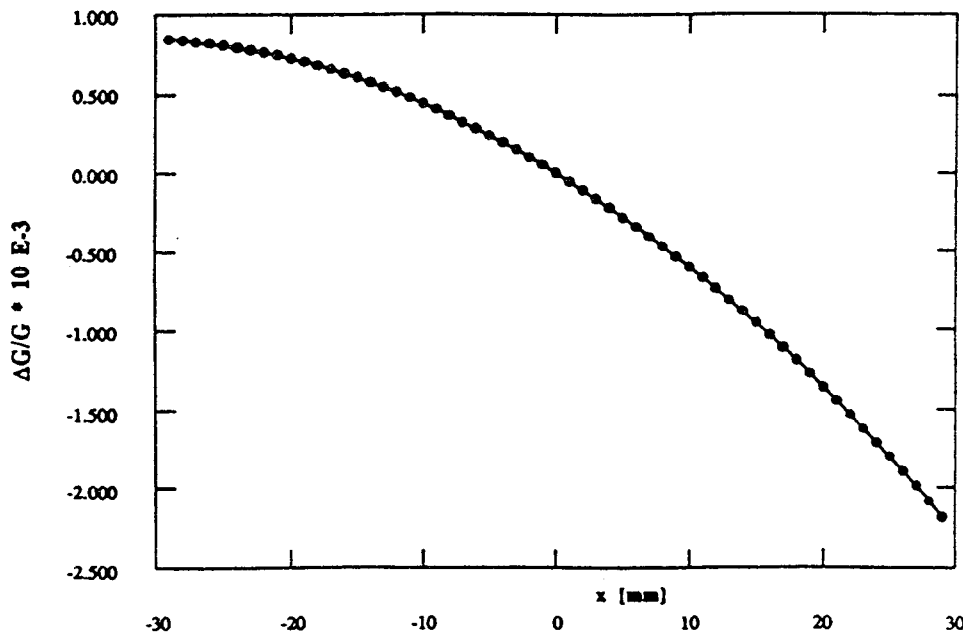
FIG. 18 – Gradient uniformity along the horizontal axis at the midplane of the quad.

In Fig. 18 the gradient variation in terms of $\Delta G/G_0$, where G_0 is the gradient at the quadrupole centre $(G_0=5.268$ T/m$)$, is reported. Fig. 19 shows the gradient variation along the

vertical axis with respect to the gradient value at the quad centre. If one compares the slopes of the above curves, clearly can note an asymmetry. To understand the cause of such a kind of asymmetry, half quadrupole has been simulated by means of Pandira and two cases have been run:

1) a completely symmetric quadrupole where the flux generators have exactly the same strength;

2) a configuration where the flux generators laying on the vertical axis have the nominal strength and the flux generators on the horizontal axis have a B_r–H_c curve respectively shifted – 4% for the right flux generator and +4% for the left one with respect to the nominal one (B_r = 8500 Gauss; H_c = 8300 Oe). The value ±4% has been deliberately chosen so high to better evaluate a macroscopic effect.
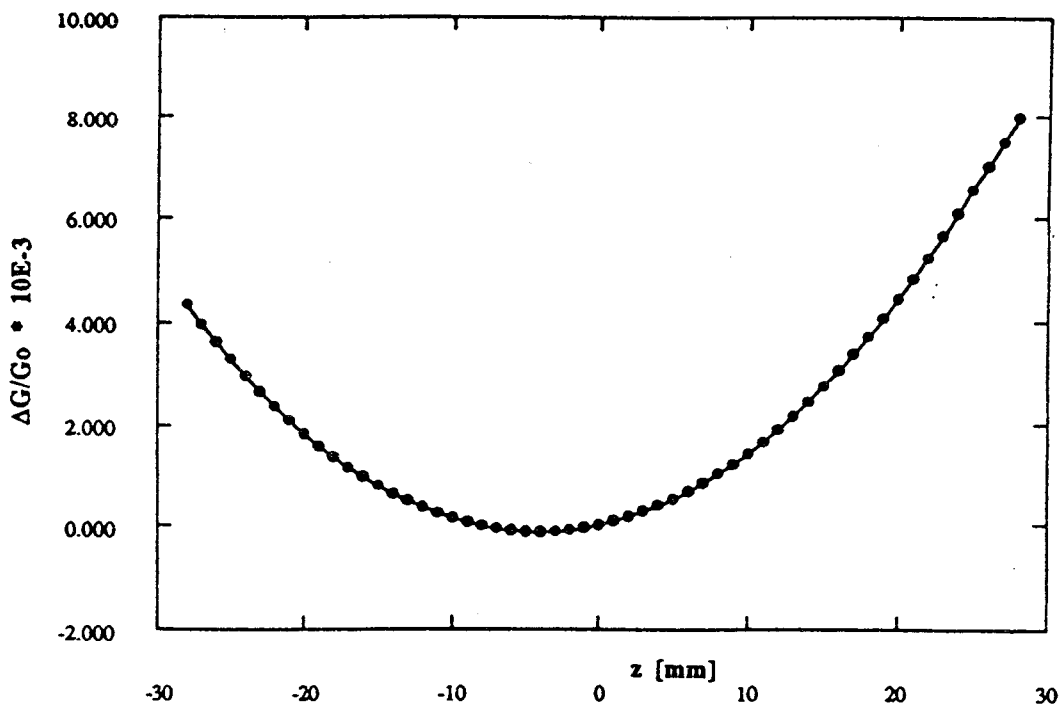

FIG. 19 – Gradient uniformity along the vertical axis at the midplane of the quad.

Fig. 20 shows the geometry simulated by Pandira where the flux lines are also plotted.

Fig. 21 shows the gradient uniformity $\Delta G/Go$ in the case of perfect symmetric flux generators and Fig. 22 shows what happens when the above unbalance is applied.This means that the quadrupole must be balanced moving the tune wedges to reach again a symmetric condition.

Fringing field measurements have been made outside the hybrid quadrupole where the strongest magnetic field is expected. The maximum value is obviously in correspondence of the medium plane with ≈ 300 Gauss near the quadrupole itself, it decreases exponentially going away from the quadrupole.

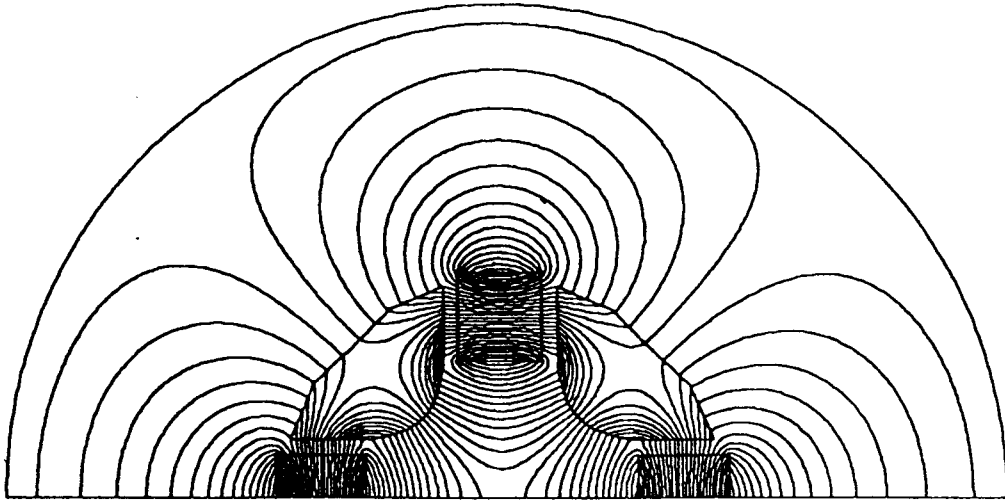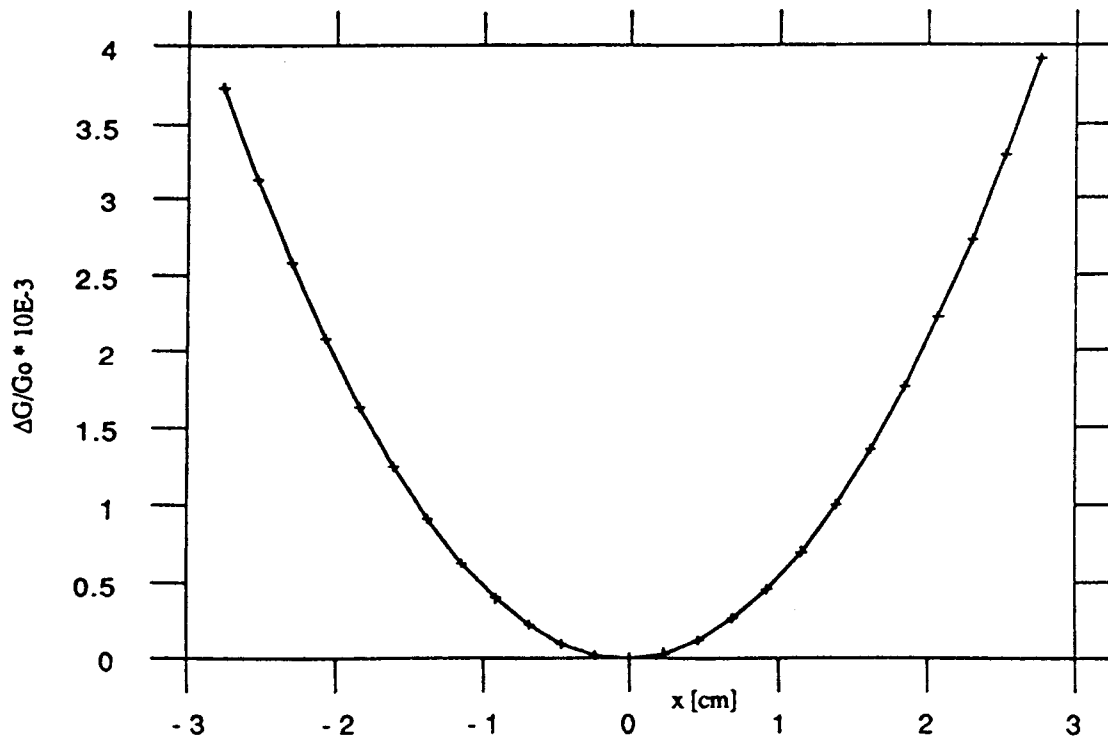**FIG. 20** – Pandira's geometry for simulating the flux generator asimmetries.

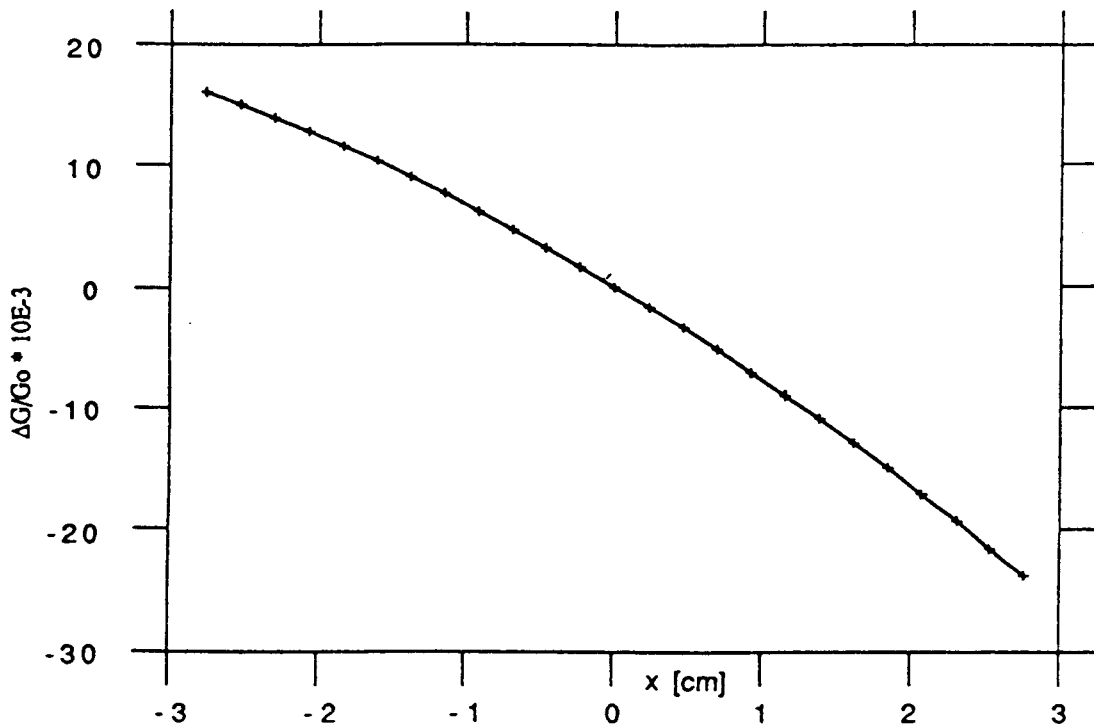**FIG. 21** – Gradient uniformity with fully symmetric flux generators.

FIG. 22 – Gradient uniformity with ±4% unbalanced flux generators.

8. – CONCLUSIONS

The magnetic measurement program is not yet completed and a deeper investigation is still needed. The major items that must be analyzed are:

-   determine the displacement of the magnetic axis with respect to the mechanical one;

-   made the harmonic content analysis by means of rotating coil;

-   balance the quad, using the tune wedges, at a fixed gradient value;

-   modify the pole profile to increase the gradient homogeneity and consequently decrease the multi–pole terms;

-   superimpose a solenoidal field and measure the total effect;

-   study the better way to shield the external fringing field.

We hope to complete the work before the end of this year, using the automatic multi–pole magnet measurement system, model 692, based on rotating coil technology, that has been ordered to Danfysik and whose delivery term is October 1992. With this system we are confident to obtain more fast and precise measurements both in the gradient and in multi–pole term analysis.

References

(1) The DAΦNE Project Team: " DAΦNE Design Criteria and Project Overview", Proc. of the Workshop on Physics and Detectors for DAΦNE, Frascati, April 9–12, 1991.

(2) The DAΦNE Project Team: " DAΦNE: The Frascati Φ–Factory " Proc. of P.A.C.1991, S. Francisco, May 6–9, 1991.

(3) M.E. Biagini et Al.: DAΦNE Lattice Update, Technical Note L–4, INFN LNF, Accelerator Division, Dec.2, 1991.

(4) "Proposal for a Φ–Factory" LNF–90/031(R)1990.

(5) M.Zobov: Energy Loss in Tapered Transitions in the DAΦNE Vacuum Chamber, Technical Note G–9, INFN LNF, Accelerator Division, Nov.12, 1991.

(6) N.I.M. 169 (1980) K.Halbach: Design of Permanent Multipole Magnets with oriented Rare Earth Cobalt Material.

(7) Asymmetric B Factory Collider Note ABC–18 (K.Halbach Sept. 25, 1990).

(8) K.Halbach et Al. " CSEM–Steel Hybrid Wiggler/Undulator Magnetic Field Studies – IEEE Trans. Nuclear Science NS–32–5 (1985).